Eye (2021) 35:17–32
https://doi.org/10.1038/s41433-020-01288-x

The ROYAL COLLEGE of OPHTHALMOLOGISTS

REVIEW ARTICLE

Optical coherence tomography (OCT) in neuro-ophthalmology

Neda Minakaran[1] · Emanuel R. de Carvalho[1,2] · Axel Petzold[1,3,4] · Sui H. Wong[1,5]

Received: 26 October 2020 / Revised: 30 October 2020 / Accepted: 4 November 2020 / Published online: 25 November 2020

Abstract

Optical coherence tomography (OCT) is a non-invasive medical imaging technology that is playing an increasing role in the routine assessment and management of patients with neuro-ophthalmic conditions. Its ability to characterise the optic nerve head, peripapillary retinal nerve fibre layer and cellular layers of the macula including the ganglion cell layer enables qualitative and quantitative assessment of optic nerve disease. In this review, we discuss technical features of OCT and OCT-based imaging techniques in the neuro-ophthalmic context, potential pitfalls to be aware of, and specific applications in more common neuro-ophthalmic conditions including demyelinating, inflammatory, ischaemic and compressive optic neuropathies, optic disc drusen and raised intracranial pressure. We also review emerging applications of OCT angiography within neuro-ophthalmology.

Introduction

Optical coherence tomography (OCT), a quick and reproducible imaging technique using low coherence interferometry to produce cross-sectional images of the retina and optic nerve head (ONH), has become one of the most valuable tools employed in the assessment of ophthalmic patients. Alongside advances in technology, its application in the field of neuro-ophthalmology specifically continues to expand.

OCT allows non-invasive visualisation of the anatomy of the most anterior part of the visual pathway, from retina to lamina cribrosa. Lesions involving the pre-laminar area can be assessed with spectral domain (SD-OCT) and enhanced depth imaging OCT (EDI-OCT) of the ONH. Beyond this, afferent visual pathway lesions involving the optic nerve, chiasm or tracts can lead to visible axonal loss caused by direct retrograde axonal degeneration. OCT imaging can capture and quantify axonal loss through measurements of retinal nerve fibre layer (RNFL) thickness, and neuronal damage through measurements of ganglion cell layer (GCL) or combined ganglion cell layer-inner plexiform layer (GCIPL) thickness. The strict anatomical structure of the retina and maintenance of retinoscopic organisation with the afferent visual pathway [1], as described in Table 1, increases the utility of OCT in evaluating central nervous system pathology.

In this review, we discuss the imaging parameters useful in the assessment of neuro-ophthalmic conditions, pitfalls to be aware of, and describe specific neuro-ophthalmic conditions where OCT imaging can help with diagnosis, management and follow-up.

Imaging the optic nerve head (ONH) and peripapillary retinal nerve fibre layer (pRNFL) thickness

OCT imaging of the ONH can be undertaken in two or three dimensions (2D or B-scan and 3D or volume scan). The OCT software can construct an ONH topographical map (Fig. 1) which can be used to quantify parameters such as ONH diameter, depth and diameter of the central cup, and thickness of the neuroretinal rim. Qualitative assessments can also be made of structural abnormalities such as optic nerve pits, tumours, optic disc drusen (ODD) and choroidal neovascularisation (CNV). EDI-OCT is beneficial for analysing the deeper structure of the ONH up to the level of the lamina cribrosa.

✉ Neda Minakaran
neda.minakaran@gmail.com

1 Moorfields Eye Hospital NHS Foundation Trust, London, UK

2 Department of Ophthalmology, University Medical Centre, University of Amsterdam, Amsterdam, The Netherlands

3 Neuro-ophthalmology Expertise Centre, University Medical Centre, University of Amsterdam, Amsterdam, The Netherlands

4 UCL Institute of Neurology, Queen Square, London, UK

5 Guys and St Thomas' NHS Foundation Trust, London, UK

The peripapillary retinal nerve fibre (pRNFL) thickness is a measure that can be used to quantify axonal integrity in pathological processes involving the optic nerve. Technical details are outlined in Table 2. Figure 2 shows an example of a pRNFL report. Normal global average pRNFL thickness is ~105 µm with an estimated physiological loss due to aging of about 0.017% per year from age 18 years onwards, equating to a 10- to 20-µm loss over a period of 60 years [2].

Table 1 Anatomy of the anterior visual pathway.

Light energy reaching retina is converted by photoreceptors into an electrochemical signal
Signal is relayed to retinal ganglion cells via bipolar, horizontal and amacrine cells
Axons of ganglion cells travel in retinal nerve fibre layer (RNFL) and converge at optic nerve head (ONH): - Foveal ganglion cell axons travel to temporal aspect of optic nerve in papillomacular bundle (caeco-central projections) - Temporal ganglion cell axons form arcuate bundles that travel above and below the fovea, crossing the horizontal meridian in a small delta area behind the foveola, finally entering the superotemporal and inferotemporal aspects of the optic nerve - Nasal ganglion cell axons enter the nasal portion of the optic nerve
Retinal ganglion cell axons travel posteriorly through the lamina cribrosa where they become myelinated and are called the optic nerve
Distal to proximal rearrangement of positions of the ganglion cells axons occurs in the first section of the optic nerve: - Macular ganglion cell axons move to the optic nerve centre - Peripheral temporal fibres become positioned more temporally, both superior and inferior to the macular fibres - Nasal fibres remain in the nasal past of the optic nerve
The two optic nerves reach the optic chiasm, typically located 10 mm above the pituitary gland, in the sella turcica within the sphenoid bone
Decussation of axons from the optic nerves takes place in the chiasm
Each optic tract contains axons from the ipsilateral temporal retina and the contralateral nasal retina
Fibres synapse in the ipsilateral lateral geniculate nucleus (LGN)

Imaging the macula and macular ganglion cell-inner plexiform layer (mGCIPL) thickness

Aside from detailed visualisation of macular structure, macular OCT scans offer the possibility to conduct manual and automated segmentation analysis of macular ganglion cell layer (mGCL) and inner plexiform layer (mIPL) densities. Technical details are outlined in Table 2. Figure 3 shows an example of a mGCL thickness map report. Both mGCL and combined mGCIPL thickness values have revolutionised the evaluation of optic neuropathies.

Pitfalls to be aware of in OCT assessment

As with any technology, there are limitations, pitfalls and potential errors that must be considered, especially when using derived measurements in clinical decision-making. Foremost, different OCT machines have different measurement protocols and so patients must be reviewed on the same machine using the same scanning protocol for accurate longitudinal comparisons to be made. Secondly, all OCT measurements are compared to a normative database. Often these normative databases are made up of Caucasian middle-aged subjects, and as such this must be considered when evaluating measurements from a patient not in this demographic, for example a child or a patient of different ethnicity.

Interpretation of automated OCT measurements need to take into account potential artefacts. The centre of the fovea on OCT may differ from the retinal locus of fixation [3, 4] and deviations of 60 ± 50 µm between fixation and the

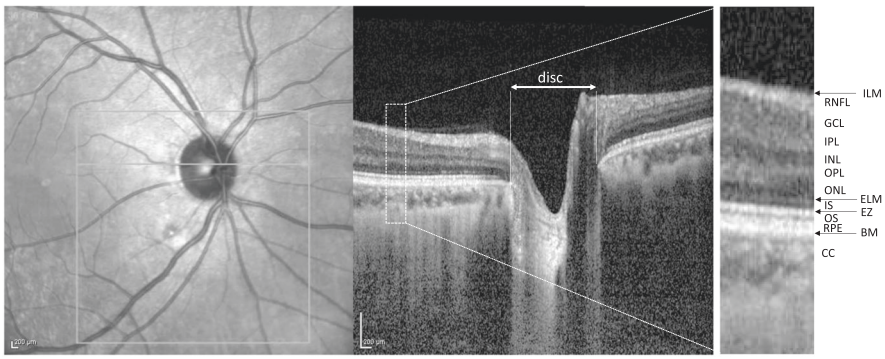

Fig. 1 Horizontal spectral-domain optical coherence tomography (SD-OCT) B-scan images of the optic nerve head (ONH) in a healthy 33-year-old female referred for assessment of non-pathological retinal pigmentary changes. The diameter of the optic disc is defined as the distance between the edges of the retinal pigment epithelium (RPE). The perpendicular orientation of the retinal nerve fibre layer (RNFL) is lost as the nerve fibres blend with the optic nerve head. BM Bruch's membrane, EZ ellipsoid zone, ELM external limiting membrane, ILM internal limiting membrane, CC choriocapillaris, OS outer segment, IS inner segment, ONL outer nuclear layer, OPL outer plexiform layer, INL inner nuclear layer, IPL inner plexiform layer, GCL ganglion cell layer.

Table 2 Technical details of OCT parameters used in the assessment of neuro-ophthalmic patients.

Peripapillary retinal nerve fibre (pRNFL) thickness analysis	Macular ganglion cell (mGCL) /inner plexiform layer (mIPL) thickness analysis
Circular cross-sectional retina scan obtained at diameter of 3.4–3.5 mm, centred around the optic nerve head (ONH)	Retinal layer segmentation required – different OCT manufacturers use different methods
Spectralis SD-OCT (Heidelberg Engineering, Heidelberg, Germany): average pRNFL thickness displayed in four quadrants. Temporal, superior, nasal and inferior and sectoral thicknesses are measured at each of the 12 clock-hours or in 16 equal sectors	Spectralis SD-OCT: offers possibility of conducting automated segmentation of perifoveal volumetric macular scans, (usually 49 B-scans 30 microns apart, 1024 A scans). Separately segments mGCL and mIPL
Cirrus HD-OCT (Carl Zeiss Meditec, Jena, Germany): deviation map generated where RNFL measurements are compared at each pixel with age-matched normative database, and location under lower 95% of normal range highlighted. Quantitative optic nerve head parameters are provided in the centre panel of the scan report	Cirrus HD-OCT: acquires an ellipse centred on the fovea with a vertical radius of 2 mm and horizontal radius of 2.4 mm, providing a combined measurement of mGCL and mIPL
Other devices display the RNFL thickness as colour-coded thickness maps of the entire peripapillary region (useful in the assessment of small, localised areas of thinning outside the sampling location)	RTVue OCT (Optovue, Fremont, US) captures a 7 mm^2 area centred 1 mm temporal to the fovea. Ganglion cell complex (GCC) measurements can be made (RNFL + GCL + IPL)

centre of the foveal avascular zone can occur [5]. For correct analysis, accurate placing of the measurement area should be checked and amended manually if necessary [6].

OCT segmentation software algorithm automatically detects the pRNFL and mGCIPL. In some cases, particularly in eyes with ocular pathology or in scans of poor image quality, the software can fail. Again, manual correction should be done to improve the accuracy and reproducibility of the measurements [6]. This may not be possible with severe retinal pathology. The introduction of eye tracking and retest software has improved reproducibility of RNFL measurements [7].

Repeatability of automated segmentation measurements has been demonstrated to vary across different OCT devices and depends on the specific scan protocol and algorithm software updates [8]. As described earlier, patients should be monitored consistently using similar OCT methodologies. The presence of ocular disorders and poor visual acuity may result in fixation errors and induce measurements that appear variable over time [9]. Likewise, assessment of retinal thickness should be limited to the area encircling the parafoveal macular rim [10].

The importance of distinguishing artefacts from true pathological changes cannot be understated, not only to ensure optimum patient care but also to avoid invasive and costly investigations.

Neuro-ophthalmic conditions

Multiple Sclerosis (MS) and demyelinating optic neuritis (MSON)

The earliest use of OCT in neuro-ophthalmology was in 1999 where Parisi and colleagues reported pRNFL thinning on OCT in MS patients with previous MSON [11]. In the acute phase of MSON, ONH swelling due to axoplasmic flow stasis in the inflamed optic nerve may be demonstrated on OCT and the elevated pRNFL measurements used to objectively quantify the swelling [12]. pRNFL thickening may also be seen in MSON where there is no clinically evident ONH swelling, and this may be useful in detecting optic neuritis flares in clinic [13]. Typically, 3 months after the acute episode of MSON, pRNFL atrophy develops which again can be quantified using OCT measurements demonstrating pRNFL thinning, most evidently in the temporal pRNFL region [14].

Due to the potentially elevated pRNFL measurements initially, followed by thinning some weeks to months later, it can be challenging to rely on pRNFL thickness to track structural changes in axonal integrity. Furthermore, there is an OCT floor effect, whereby mean pRNFL values do not generally reduce below 30 µm regardless of extent of optic nerve injury, making it difficult to detect appreciable change in severe optic atrophy or recurrent optic neuritis [15]. OCT-mGCL or mGCIPL volume and thickness analysis has been shown to be a more sensitive and reliable measure of retrobulbar neuroaxonal injury. mGCIPL thinning occurs earlier in the time course of acute ON (after about 2 weeks), even whilst the RNFL remains oedematous, thus providing an early indication of retinal ganglion cell dropout and possible permanent visual dysfunction [16]. Whilst lower pRNFL values have been shown to correlate with reduced visual acuity, contrast sensitivity, visual field mean sensitivity and colour vision mean testing scores [17, 18], mGCIPL thickness correlates better with these measures of visual dysfunction, as well as quality of life measures, disability and MRI findings [19, 20]. Overall OCT is helpful for prognostication after MS-related relapses.

MS patients can experience substantial subclinical disease activity, and even in the absence of clinical MSON

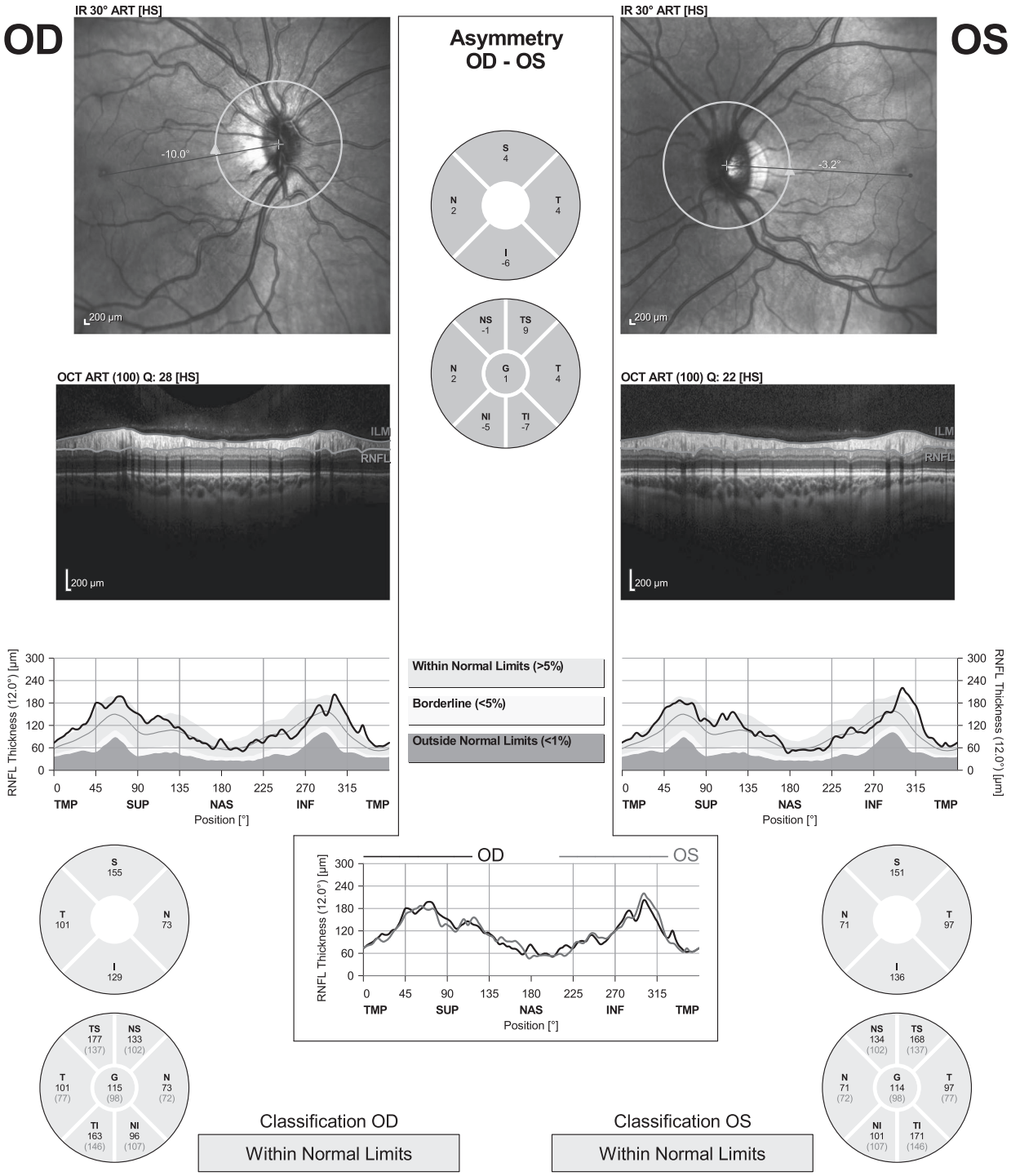

Fig. 2 Spectral-domain optical coherence tomography (SD-OCT) peripapillary retinal nerve fibre layer (pRNFL) report in a healthy asymptomatic 27-year-old female. The RNFL thickness falls within normal range in all segments (TMP temporal, SUP superior, NAS nasal, INF inferior).

events, can develop progressive pRNFL and mGCIPL thinning [21, 22]. A meta-analysis comparing 1,667 MSON eyes and 4,109 MS non-ON eyes to 1,697 eyes from healthy control subjects found significant pRNFL and mGCIPL thinning in both MSON eyes (mean difference −20 µm and −16 µm respectively) and MS non-ON eyes (mean difference −7 µm and −6 µm respectively) relative to control eyes [23]. Without additional MRI or electrodiagnostic data, the meta-analysis cannot conclude whether the finding in the MS non-ON eyes is a manifestation of a primary

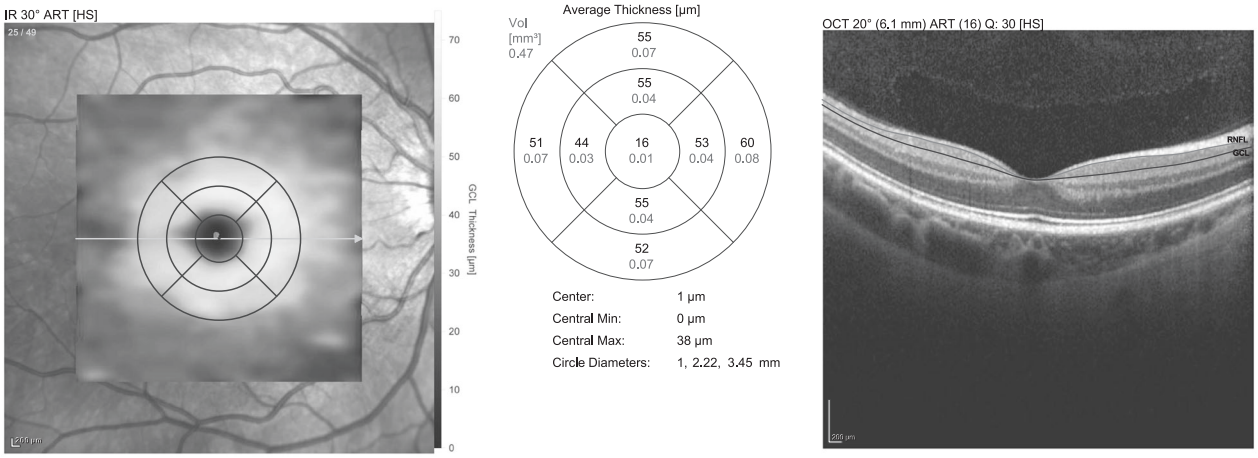

Fig. 3 Spectral-domain optical coherence tomography (SD-OCT) macular ganglion cell layer (mGCL) thickness map report in a healthy asymptomatic 27-year-old female. The report for the right eye shows normal macular ganglion cell layer (mGCL) density and thickness (1, 2.22 m 3.45 mm volume scan) after segmentation.

neurodegenerative component of MS, or whether it is due to retrograde transsynaptic degeneration from pathology of the posterior visual pathway. These data come from smaller sized, multimodal cohort studies and case reports [24]. However, the finding does suggest that OCT could be used in the measurement of disease activity in MS, potentially reducing the need for frequent MRIs. This is further supported by the fact that reduced pRNFL and mGCIPL values have been shown to correlate with other surrogate markers used to monitor disease activity such as MRI-measured brain atrophy [25, 26], spinal cord lesions [27] and neurological disability scores [25, 26, 28–30]. Figure 4 demonstrates findings in an MS patient with post-chiasmal demyelination with mGCL density measurements mirroring the visual field defect.

Microcystic macular changes detected on retinal OCT has been a recent area of interest since first reported in patients with demyelinating optic neuropathy in 2012 by Gelfand et al. [31]. Small hyporeflective spaces within the inner nuclear layer (INL) in the parafoveal region of the fovea are characteristic, with sparing of the fovea itself, which would otherwise be involved in vascular leakage. Microcystic macular changes and thickening of the INL have been shown to be associated with disease activity and worse disability in MS [32]. However, microcystic macular change is not unique to MS and can be observed across a variety of optic neuropathies, including non-inflammatory aetiologies such as compressive optic neuropathy [33]. With several studies showing no corresponding dye leakage on fluorescein angiography [34, 35], it is likely that these changes are due to retrograde axonal degeneration and that loss of retinal Müller cell function plays a role in microcyst formation [36]. The literature uses the terms ‘microcystic changes’, ‘retrograde maculopathy’, ‘microcystic macular oedema (MMO)’, and microcystic macular edema (MME). None of these terms distinguish transient from permanent changes. Terminology and understanding of this novel observation are still evolving.

Neuromyelitis Optica Spectrum Disorder (NMOSD)

Whilst pRNFL and mGCIPL thinning is typical in optic neuritis generally, the degree and pattern of loss may help with differentiating underlying aetiology. It has been shown that ON related to NMOSD leads to more pronounced thinning of the pRNFL and mGCIPL than in MSON [37, 38]. The distribution of pRNFL thinning also differs, with NMO-ON preferentially involving the inferior and superior quadrants, versus the temporal quadrant which is more typically affected in MS [37]. Patients with NMOSD do not seem to suffer the progressive pRNFL atrophy that occurs in MS independent of ON episodes [39], as described earlier, with damage appearing to be attack-related, although some studies have shown the mGCIPL to undergo progressive thinning [40]. This seems to be specific for aquaporin4 IgG positive NMOSD, whereas myelin-oligodendrocyte-glycoprotein (MOG) IgG positive NMOSD patients demonstrate a more similar pattern to MS patients [41]. The reason for this is not clear, and certainly the time course in NMO-ON and MOG-ON is less well understood than in MSON, with the relationship between severity of atrophy observed and loss of visual function also being less well correlated. Microcystic macular change is also seen more frequently in NMOSD patients (20–26%) than in MS patients (1–5%) [37, 42], and INL measurements are thicker in NMOSD versus MS patients [43, 44]. This may be a reflection of the severity of optic neuropathy and the resultant retrograde degeneration. Figure 5 demonstrates progressive pRNFL and mGCL thinning in a patient with NMO after right eye optic neuritis.

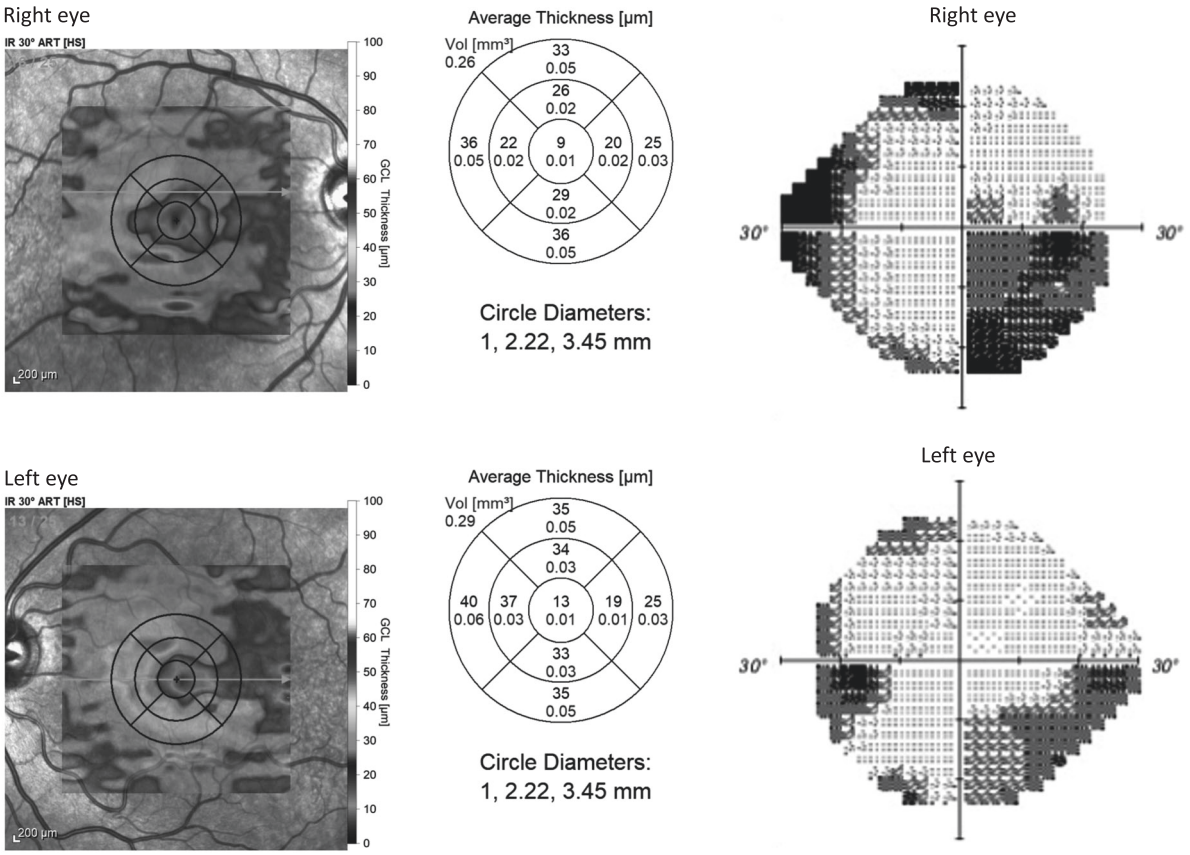

Fig. 4 A 36-year-old male with relapsing-remitting multiple sclerosis (MS) presented with visual complaints and was found to have a right inferior incongruous visual field defect. The spectral-domain optical coherence tomography (SD-OCT) macular ganglion cell layer (mGCL) analysis shows a corresponding pattern of left hemiretinal loss. This is indicative of left-sided post-chiasmal demyelination (left optic tract or radiation), with MRI images confirming left optic radiation volume loss.

Optic disc drusen (ODD)

ODD are acellular intracellular and extracellular deposits located in the optic nerve that may become calcified over time. Whilst superficial ODD can be detected on clinical examination, distinguishing buried optic disc drusen from optic disc swelling remains a clinical challenge. Ancillary tests including fundus autofluorescence, computer tomography, fluorescein angiography and B-scan ultrasonography are used to help distinguish between the two. These do have their limitations, however. B-scan ultrasonography, for example, whilst traditionally viewed as the 'gold-standard' test for detection of buried ODD, is unable to detect non-calcified drusen or peripapillary hyperreflective ovoid mass-like structures (PHOMS) [45]. Resolution is relatively poor, making it difficult to monitor drusen progression [45]. Furthermore, B-scan ultrasonography does not give information regarding the neuroaxonal integrity of optic nerve and retinal structures, and as such does not allow prognostication with regards to visual outcomes in patients with ODD [46].

OCT, specifically EDI-OCT, has earned its place as not only a useful complement but as a potential competitor as the gold-standard for diagnosis and analysis of ODD. Prior to mainstream use of EDI technology, there was much variability in the literature with regards to ODD morphology on OCT. Early studies focussed on RNFL thickness differences between ODD and disc oedema [47, 48], but this was found to be unreliable [49]. Other OCT features described in the literature included ODD appearing as highly reflective round sub-retinal structures with well-defined margins displacing the adjacent tissue [47], and a 'lazy V' pattern or 'lumpy bumpy' internal contour of the subretinal hyporeflective space helping to distinguish between ODD and papilloedema [50, 51]. However, the hyporeflective space was actually an imaging artefact and a by-product of poor-penetrance inherent to early generations of OCT [45].

The improved penetrance afforded by EDI-OCT technology now enables quantification of drusen size, delineation of drusen borders and assessment of the integrity of adjacent retinal structures. The Optic Disc Drusen Studies

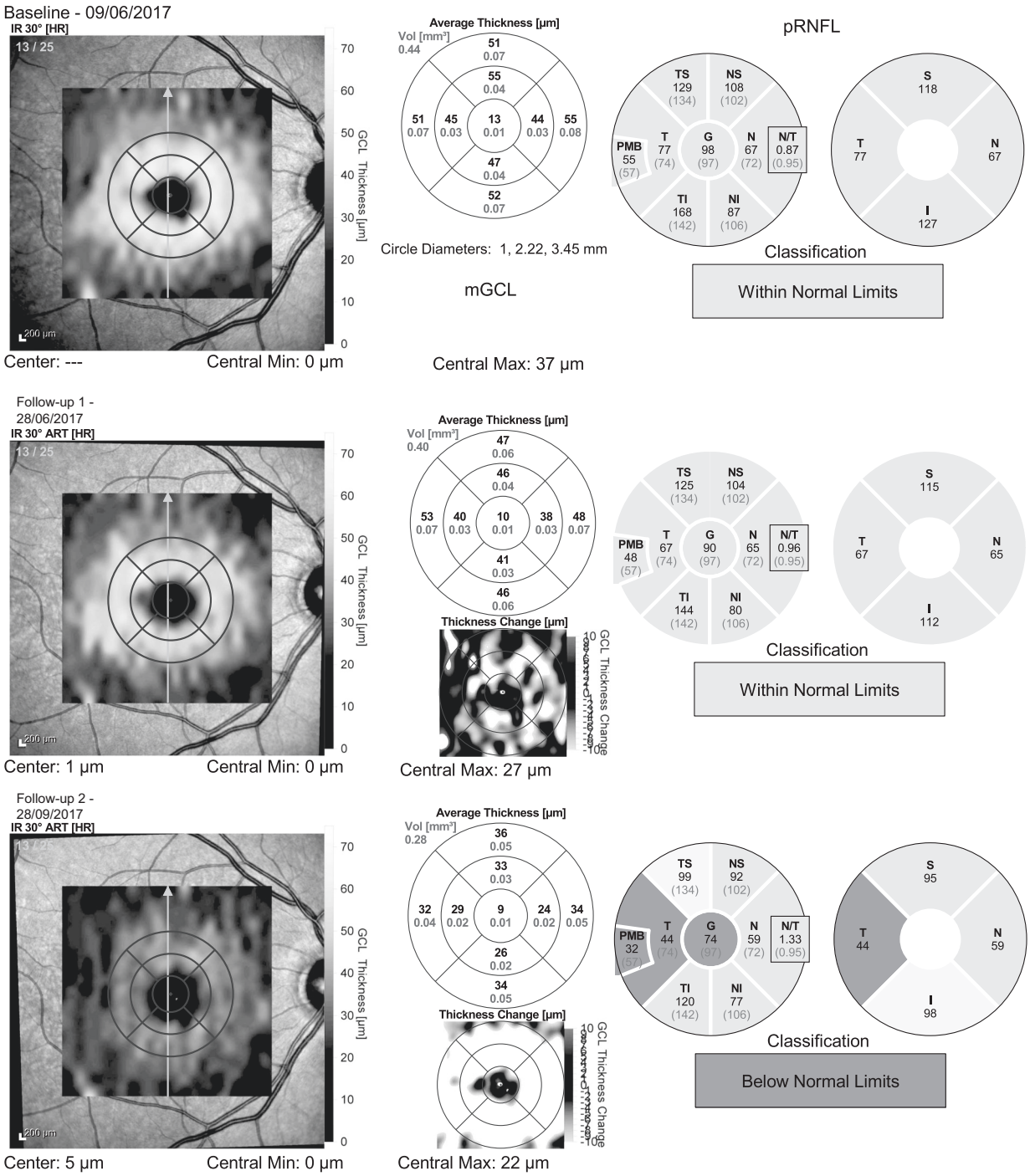

Fig. 5 A 44-year-old female with sero-negative neuromyelitis optica (NMO) presented with right eye optic neuritis. The spectral-domain optical coherence tomography (SD-OCT) imaging demonstrates progressive thinning of the peripapillary retinal nerve fibre layer (pRNFL) and macular ganglion cell layer (mGCL) after presentation, shown here at 3 weeks and 3 months post episode.

Consortium has published guidelines for the assessment of ODD [52]. They define ODD as hyporeflective structures always located above the lamina cribrosa, with a full or partial hyperreflective margin, often most prominent superiorly (Fig. 6). Blood vessels, which appear as elongated tube-like structures, are distinguished from ODD as they lack the hyperreflective signal around them. ODD are often seen as conglomerates of smaller ODD with internal reflectivity within the signal-poor core. Hyperreflective horizontal lines might represent early ODD but should not be diagnosed as ODD.

EDI-OCT has been shown to have significantly higher ODD detection rate than B-scan ultrasonography [53]. Furthermore, the size and type of ODD classified by EDI-

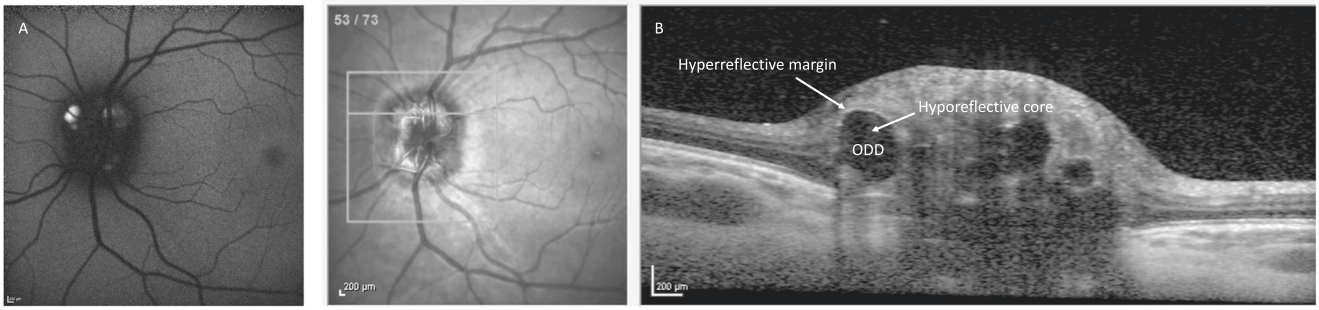

Fig. 6 OCT imaging of optic disc drusen (ODD) in a 48-year-old male. Optic disc drusen (ODD) are visible on fundus autofluorescence (**a**) with corresponding morphology demonstrated on enhanced depth imaging spectral-domain optical coherence tomography (EDI SD-OCT) (**b**). ODD are seen as signal-poor structures with a partial hyperreflective margin.

OCT have been shown to correlate with visual field defects. Specifically, confluent ODD have been associated with worse mean deviation scores on visual fields testing [54]. Some studies have suggested that EDI-OCT ODD volumes correlate with structural optic nerve head damage and functional deficits among patients [55]. The capability of EDI-OCT to quantify ODD volume, and additional ability of OCT to measure neuroaxonal changes in the retina, will enable the monitoring of ODD progression and potentially provide guidance with regards to risk factors for vision loss in ODD patients.

Peripapillary hyper-reflective ovoid structures (PHOMS)

Peripapillary hyper-reflective ovoid mass-like structures (PHOMS) were originally described in patients with ODD [47–49] and were thought to represent precursors or variants of ODD [54]. However, as explained by the Optic Disc Drusen Studies Consortium, PHOMS, unlike ODD, are hyperreflective without a sharp outer margin or hyporeflective core [52] (Fig. 7). They are neither visible on fundus autofluorescence nor on B-scan ultrasonography, and they can be found on OCT in patients with papilloedema without ODD [52]. They are thought to represent disruption of retinal layers caused by local axoplasmic build-up [45], with the histopathology of papilledema suggesting that PHOMS might correspond to the lateral bulging of distended axons into the peripapillary retina [52]. Of note, PHOMS can also be seen in crowded discs, or "pseudo-papilloedema" and therefore are not useful as a distinguishing feature for papilloedema.

Idiopathic intracranial hypertension and papilloedema

Idiopathic intracranial hypertension is a condition of unknown aetiology, typically associated with obesity, that can lead to headaches, optic disc swelling and, in some cases, permanent visual loss [56]. OCT allows accurate and objective monitoring of this condition, not only with respect to the degree of optic disc swelling present, but also with quantification of resultant optic neuropathy.

The OCT pRNFL measurements can be used to serially monitor the degree of optic disc swelling present over consecutive visits (Fig. 8), which is a far more reliable and sensitive method of evaluating change than comparisons of clinician-assessed Frisén grades [57, 58]. Furthermore, whilst reduction in disc swelling and pRNFL thickness may be a result of treatment success or general improvement, it may also be a result of worsening axonal loss from disease progression. OCT mGCIPL thickness measurements play a critical role here for distinguishing between these two entities. Reduction in pRNFL thickness with preserved mGCIPL thickness indicates treatment success with preservation of the neuroaxonal structure, whereas reduction in both indices indicates worsening optic neuropathy and treatment failure or fulminant IIH.

EDI-OCT may demonstrate PHOMS in papilloedema. EDI-OCT also enables visualisation of Bruch's membrane, and peripapillary deformations of Bruch's membrane surrounding the neural canal due to a differential pressure between the retrobulbar optic nerve and vitreous cavity can also be useful in the diagnosis and management of patients with intracranial hypertension. In raised intracranial pressure, there can be an upward deflection of Bruch's membrane towards the vitreous [59, 60] (Fig. 9), and after treatment there can be normalisation to a downward deflection of the Bruch's membrane complex [59, 61]. There is anecdotal evidence that this can be seen straight after lumbar-puncture induced lowering of intracranial pressure, much sooner than fundal appearances of papilloedema, and indeed even OCT pRNFL thickness changes [62, 63].

OCT is also helpful in differentiating between vision loss in papilloedema due to optic neuropathy, or due to retinopathy such as subretinal macular fluid or choroidal folds. Decreased vision due to the latter two are generally more benign and reversible, and treatment may not need to be as aggressive as is the case in optic neuropathy [64].

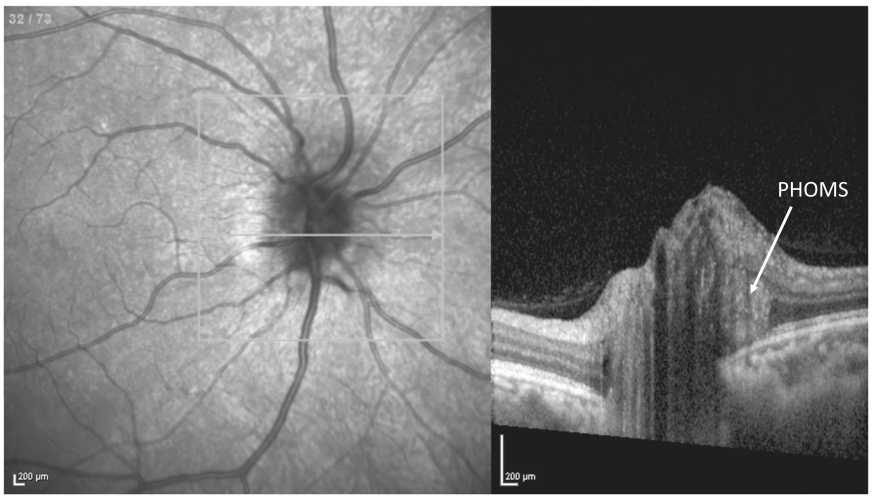

Fig. 7 OCT imaging of peripapillary hyper-reflective ovoid mass structure (PHOMS) in a 37-year-old male who also has optic disc drusen (ODD). Enhanced depth imaging spectral-domain optical coherence tomography (EDI SD-OCT) shows a peripapillary hyper-reflective ovoid mass structure (PHOMS).

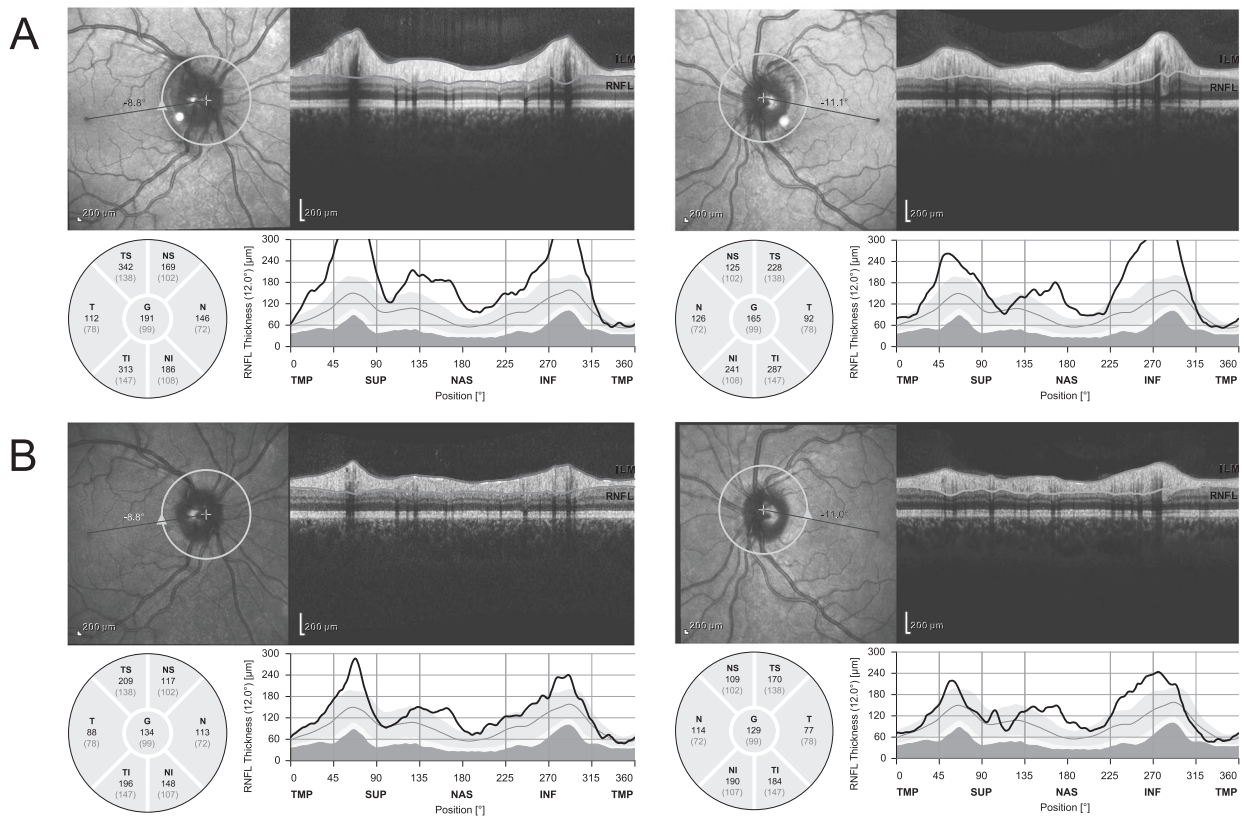

Fig. 8 A 23-year-old female presented with headaches and was found to have bilateral optic disc swelling, and after investigation was diagnosed with idiopathic intracranial hypertension (IIH). Spectral domain optical coherence tomography (SD-OCT) imaging demonstrates bilateral perpipapillary retinal nerve fibre layer (pRNFL) thickening at presentation (**a**). There was improvement in symptoms and pRNFL thickening after commencement of acetazolamide and weight loss strategies at 4 months after diagnosis (**b**).

Lastly, functional overlay is not uncommon in patients with IIH. OCT analysis of mGCIPL thickness as an objective marker of established optic neuropathy provides additional insight, along with the results of other tests such as kinetic perimetry and visual evoked potentials, as to whether functional overlay may play a role in explaining poor visual function.

Anterior ischaemic optic neuropathies (AION)

OCT plays a similar role in the assessment of ischaemic optic neuropathies as it does in assessment of optic neuritis. Acutely, optic disc swelling can be diagnosed and quantified using pRNFL thickness measurements. Within 2 months, 80% of patients subsequently show pRNFL

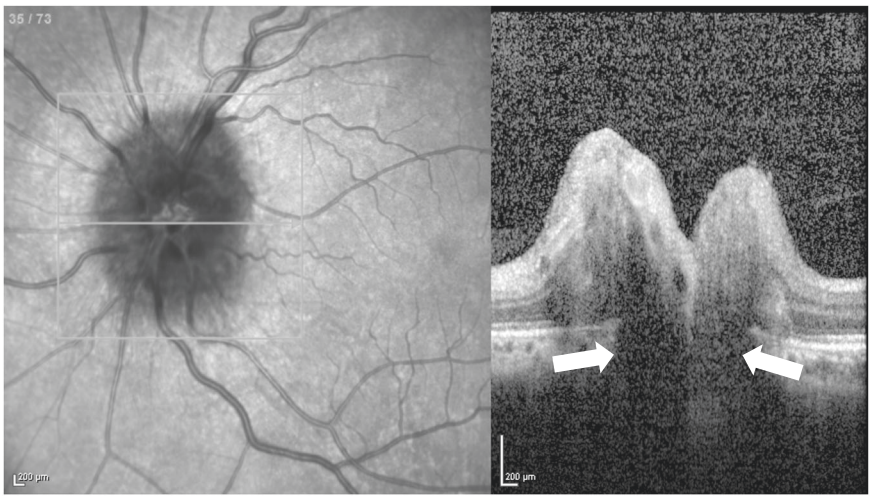

Fig. 9 A 47-year-old male presented with headaches and was found to have bilateral optic disc swelling, after investigation deemed secondary to raised intracranial pressure. Enhanced depth imaging spectral-domain optical coherence tomography (EDI SD-OCT) demonstrates upward deflection of Bruch's membrane (arrows).

thinning, with progressive thinning and thus optic disc atrophy occurring between months 2 and 4, with stability typically reached at month 6 [65–67]. As with optic neuritis, thinning of the mGCIPL has been shown to occur much earlier than pRNFL thinning. It can occur as early as 2.2 days after onset of symptoms, and thinning of the mGCIPL density has been shown to be present in 62.5% of eyes at presentation [68]. Longitudinal assessment of the mGCIPL layer offers a reliable and objective tool in monitoring of these patients (Fig. 10). Furthermore, the pattern of mGCIPL loss often indicates the degree and pattern of visual field loss [69–71], which in non-arteritic ischaemic optic neuropathy (NA-AION) is often altitudinal.

OCT can also be used to distinguish between a chronic branch retinal artery occlusion and NA-AION. Whilst both can cause an altitudinal visual field defect and corresponding pallor of the optic nerve in the post-acute phase, retinal artery occlusions will cause thinning of the entire inner retina including the INL, whereas in NA-AION the thinning will be limited to the pRNFL and mGCIPL. As retinal artery occlusions require a thromboembolic work-up and NA-AION do not, it is important to clinically distinguish between the two. In clinical practice it is helpful to compare the visual field with the macular OCT. The anatomical defect seen in the mGCIPL thickness should match the functional deficit depicted in the visual field.

Compressive optic neuropathies

Compression of the anterior visual pathway most commonly occurs at the level of the optic chiasm, for example by pituitary lesions, but compression of the optic nerve can also occur elsewhere, for example by meningiomas or in the orbit by the enlarged muscles of thyroid eye disease. OCT plays a role, not only in diagnosis and monitoring of compression, but also in prediction of visual outcomes after decompression surgery.

Compression causing optic nerve damage can be detected on OCT earlier than may be visible on fundoscopy. Both pRNFL and mGCIPL thinning can be detected and quantified on OCT imaging, with mGCIPL analysis being particularly sensitive for detecting compressive optic neuropathy. Not only may mGCIPL thinning occur earlier than pRNFL thinning [72], but in some studies it has also been shown to occur before standard automated perimetry changes [73, 74]. A hemianopia on perimetry can present as a hemi-macular atrophy on the OCT.

The pattern of pRNFL and mGCIPL loss may be helpful in detecting some compressive optic neuropathies. In prechiasmatic unilateral optic nerve compression, asymmetry in pRNFL and mGCIPL thickness between eyes gives a clue to the location of the compression. Lesions compressing the optic chiasm superiorly or inferiorly predominantly compress the decussating nasal fibres, resulting in retrograde RNFL loss on the nasal and temporal sides of the optic disc. This can be identified clinically as bow tie or band optic atrophy [75, 76]. Whilst multiple studies have shown patients with band atrophy to have pRNFL loss in all 4 quadrants around the optic disc, not just the horizontal band [77–81], there is greater proportional thinning nasally and temporally in patients with bitemporal hemianopia from chiasmal compression [78] (Fig. 11). The pattern of mGCIPL loss is more consistent, with binasal thinning occurring typically in chiasmal compression [73, 82]. Homonymous mGCIPL thinning is seen in optic tract and lateral geniculate nucleus injuries, not only from compressive lesions but also from vascular ischaemia or demyelination [83]. Post-geniculate lesions can also lead to homonymous mGCIPL thinning through trans-synaptic retrograde degeneration, but this OCT pattern does not occur acutely and may take over a year to develop [84].

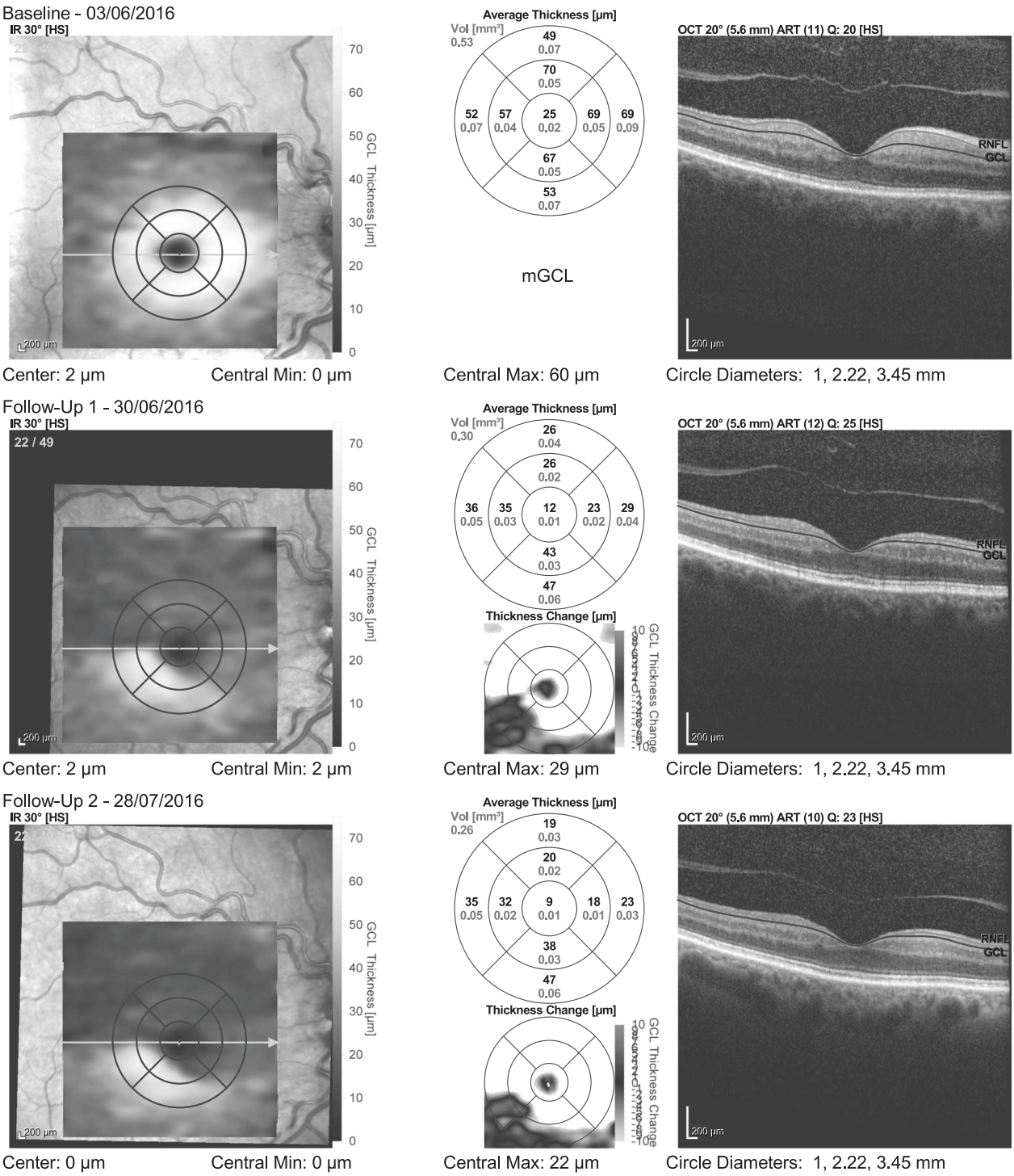

Fig. 10 A 70-year-old female presented with headache and reduced vision in the right eye. She was diagnosed with right arteritic anterior ischaemic optic neuropathy (A-AION) due to giant cell arteritis (GCA). Spectral domain optical coherence tomography (SD-OCT) imaging demonstrates progressive thinning of the macular ganglion cell layer (mGCL) from onset, shown here at 3 weeks and 8 weeks post presentation.

OCT can be helpful in differentiating compressive optic neuropathies from normotensive glaucoma. In glaucoma, pRNFL thinning tends to be vertical and the mGCIPL thinning tends to respect the horizontal meridian [82], distinct from that seen in chiasmal compressive lesions.

OCT may potentially play a role in monitoring and management decisions in paediatric intrinsic optic pathway gliomas, which are typically managed conservatively with treatment initiated on documented visual decline. However, reliably measuring visual function using visual

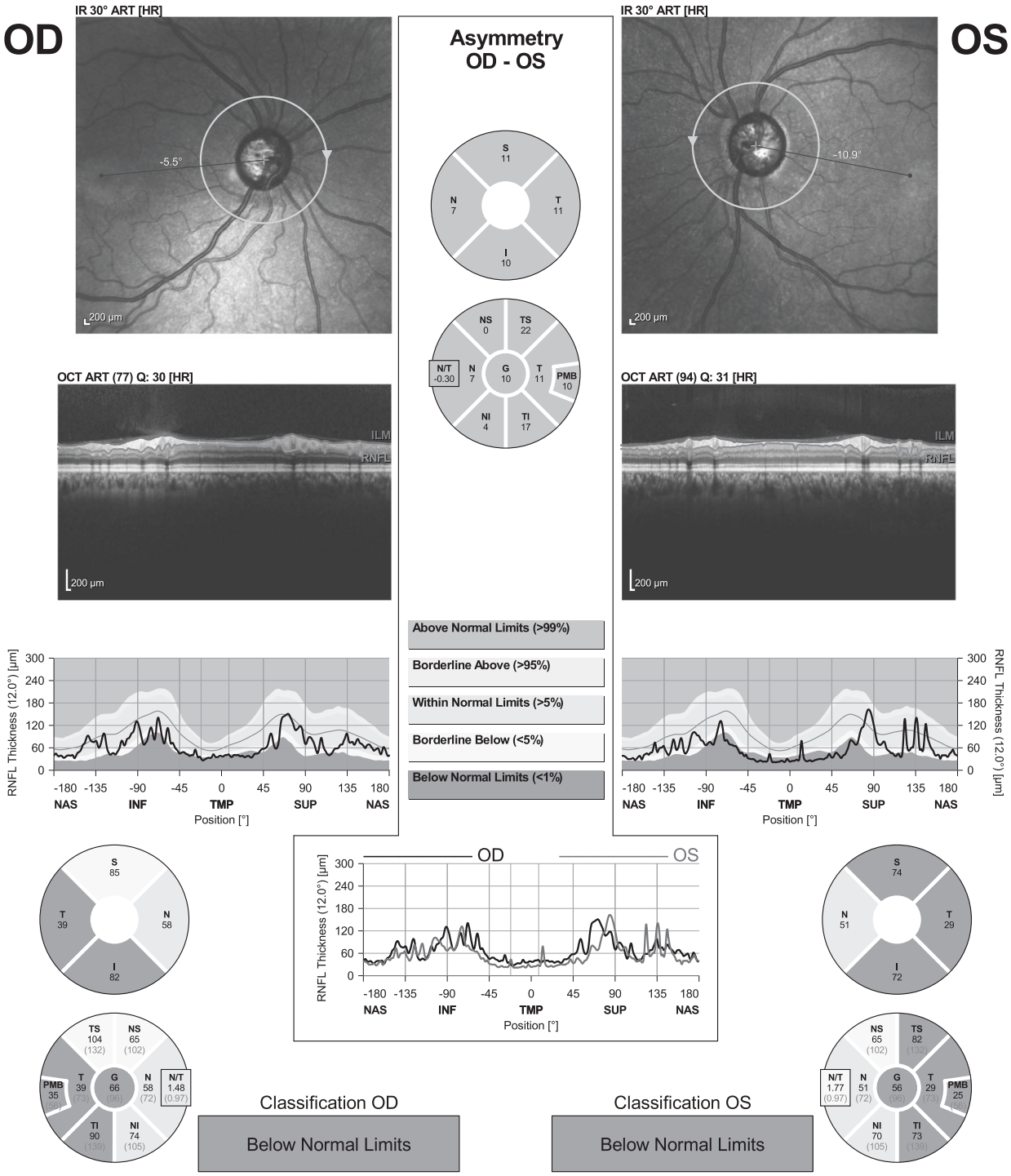

Fig. 11 A 64-year-old male with bilateral established optic neuropathy secondary to a pituitary adenoma causing compression of the optic chiasm was followed up in clinic. The spectral-domain optical coherence tomography (SD-OCT) peripapillary retinal nerve fibre layer (pRNFL) report shows bilateral pRNFL thinning, especially temporally.

acuity and visual fields in young children can be difficult, and optic nerve glioma size on MRI is poorly predictive of visual function [85]. OCT pRNFL thinning has been shown to be sensitive and specific for vision loss in this group of patients [86], although this finding has been challenged [87]. Further research is needed to fully support the use of longitudinal OCT assessments to aid therapeutic decision-making.

OCT is helpful in assessing visual dysfunction and predicting post-surgical visual outcomes in compressive optic neuropathies. Both pre-operative pRNFL thickness [62, 88] and mGCIPL thickness [74, 89, 90] should be considered,

and one parameter is not necessarily superior to the other as prediction of visual outcomes is multifactorial, depending also on lesion location, duration and severity of compression [46]. Both have been shown to correlate with visual field loss and visual outcomes post-surgical decompression, with lower chance of complete visual recovery when there is greater pRNFL and mGCIPL thinning.

Optical coherence tomography angiography (OCTA) in neuro-ophthalmology

OCT technology continues to improve and evolve, and the availability of optical coherence tomography angiography (OCTA) is one such advancement. OCTA provides non-invasive imaging of the perfused vascular network of the neurosensory retina and optic nerve head. Technical details are outlined in Table 3.

In neuro-ophthalmology, OCTA assessment of the peripapillary radial capillary network, a layer not visible on traditional fluorescein angiography [91], can be useful. Peripapillary radial vessels are located in the RNFL, superficial to the inner retinal plexus. These vessels are susceptible to fluctuations in intraocular pressure and their density has been shown to correlate with RNFL thickness [92]. For instance, in glaucomatous optic neuropathy, reduced perfusion, reduced vessel density and pre-laminar blood flow of the optic nerve head correlate with pRNFL, mGCIPL, visual field mean deviation, and visual field index [93]. Reduced peripapillary radial capillary network perfusion has been demonstrated in demyelinating optic neuritis [94] and ischaemic optic neuropathies [95]. The difficulty here is that OCTA is not reliable in a swollen disc. Moreover, partial reperfusion of peripapillary vascular flow has been linked to visual acuity improvement in NA-AION [96]. The association of absent focal perfusion alongside superficial peripapillary capillary dilation has been advanced as a potential diagnostic sign for arteritic AION [97]. In established cases of Leber hereditary optic neuropathy and autosomal dominant optic atrophy, reduction in peripapillary perfusion is consistently observed [98, 99].

Table 3 Technical details of optical coherence tomography angiography (OCTA).

OCTA generates motion-contrast images, that arise due to variable backscattering of light from the vascular and neurosensory tissue in the retina
Scans are performed at the same location and temporal changes are measured, permitting the differentiation of moving particles from static tissue. In the retina, movement is largely generated by red blood cells
Motion detection can be gathered by amplitude decorrelation or phase variance
Amplitude decorrelation detects differences in amplitude between two different OCT B-scans
Phase relies on emitted light wave properties and the variation of phase derived from the interception with moving objects
After Fourier transform, the OCT signal contains amplitude (intensity) and phase information
Two averaging methods are then applied to reduce background noise from normal eye movements, namely the split spectrum amplitude decorrelation technique and volume averaging
The images, with a size between 3 mm^2 to 12 mm^2, provide information from the superficial retinal plexus (including the superficial radial peripapillary capillaries and inner vascular plexus within the ganglion cell layer), the deep retinal plexus, the outer retina, and the choriocapillaris

Conclusion

OCT imaging has revolutionised neuro-ophthalmic practice and with ever advancing technology the scope for further applications will continue to expand. We have described its application in the diagnosis, monitoring and prognostication of a number of more common neuro-ophthalmic conditions, including demyelinating, inflammatory, ischaemic and compressive optic neuropathies, optic disc drusen and raised intracranial pressure. This list is not exhaustive, and there are a multitude of other neuro-ophthalmic conditions that also benefit from the capabilities that OCT imaging affords with respect to diagnosis and management. The use of computer-generated information, however, must always be reviewed for potential inaccuracies or artefacts, correctly and critically interpreted, and integrated into the clinical context. This is an exciting area in both neuro-ophthalmic research and clinical practice, and as OCT technology continues to improve, it will undoubtedly enhance our understanding of the pathophysiology of neuro-ophthalmic diseases in the future.

Compliance with ethical standards

Conflict of interest The authors declare that they have no conflict of interest.

Publisher's note Springer Nature remains neutral with regard to jurisdictional claims in published maps and institutional affiliations.

References

1. Prasad S, Galetta S. Anatomy and physiology of the afferent visual system. In: Kennard C, Leigh RJ (eds). Handbook of Clinical Neurology, Vol 102. Elsevier: Amsterdam, The Netherlands; 2011, pp 3-19.
2. Kanamori A, Escano MF, Eno A, et al. Evaluation of the effect of aging on retinal nerve fiber layer thickness measured by optical coherence tomography. Ophthalmologica. 2003;217:273–8.

3. Putnam NM, Hofer HJ, Doble N, Chen L, Carroll J, Williams DR. The locus of fixation and the foveal cone mosaic. J Vis. 2005;5:632–9.
4. El-Ashry M, Hegde V, James P, Pagliarini S. Analysis of macular thickness in British population using optical coherence tomography (OCT): An emphasis on interocular symmetry. Curr Eye Res. 2008;33:693–9.
5. Zeffren BS, Applegate RA, Bradley A, Vanheuven WAJ. Retinal fixation point location in the foveal avascular zone. Invest Ophth Vis Sci. 1990;31:2099–105.
6. Ctori I, Huntjens B. Repeatability of foveal measurements using spectralis optical coherence tomography segmentation software. Plos ONE. 2015;10:e0129005.
7. Langenegger SJ, Funk J, Toteberg-Harms M. Reproducibility of retinal nerve fiber layer thickness measurements using the eye tracker and the retest function of spectralis SD-OCT in glaucomatous and healthy control eyes. Invest Ophth Vis Sci. 2011;52:3338–44.
8. Eriksson U, Alm A. Repeatability in and interchangeability between the macular and the fast macular thickness map protocols: a study on normal eyes with Stratus optical coherence tomography. Acta Ophthalmologica. 2009;87:725–30.
9. Comyn O, Heng LZ, Ikeji F, Bibi K, Hykin PG, Bainbridge JW, et al. Repeatability of spectralis OCT measurements of macular thickness and volume in diabetic macular edema. Invest Ophth Vis Sci. 2012;53:7754–9.
10. Gilmore ED, Hudson C. Eccentricity and measurement variability and repeatability with the retinal thickness analyser. Brit J Ophthalmol. 2004;88:62–5.
11. Parisi V, Manni G, Spadaro M, Colacino G, Restuccia R, Marchi S, et al. Correlation between morphological and functional retinal impairment in multiple sclerosis patients. Invest Ophthalmol Vis Sci. 1999;40:2520–7.
12. Kupersmith MJ, Mandel G, Anderson S, Meltzer D, Kardon R. Baseline, one and three month changes in the peripapillary retinal nerve fiber layer in acute optic neuritis: relation to baseline vision and MRI. J Neurol Sci. 2011;308:117–23.
13. Pro MJ, Pons ME, Liebmann JM, Ritch R, Zafar S, Lefton D, et al. Imaging of the optic disc and retinal nerve fiber layer in acute optic neuritis. J Neurol Sco. 2006;250:114–9.
14. Costello FE, Klistorner A, Kardon R. Optical coherence tomography in the diagnosis and management of optic neuritis and multiple sclerosis. Ophthalmic Surg, Lasers Imaging. 2011;42: S28–40.
15. Ye C, Lam DS, Leung CK. Investigation of floor effect for OCT RNFL measurement. Invest Ophthalmol Vis Sci. 2011;52:176.
16. Kupersmith MJ, Garvin MK, Wang JK, Durbin M, Kardon R. Retinal ganglion cell layer thinning within one month of presentation for optic neuritis. Mult Scler. 2016;22:641–8.
17. Trip SA, Schlottmann PG, Jones SJ, Altmann DR, Garway-Heath DF, Thompson AJ, et al. Retinal nerve fiber layer axonal loss and visual dysfunction in optic neuritis. Ann Neurol. 2005;58:383–91.
18. Fisher JB, Jacobs DA, Markowitz CE, Galetta SL, Volpe NJ, Nano-Schiavi ML, et al. Relation of visual function to retinal nerve fiber layer thickness in multiple sclerosis. Ophthalmology. 2006;113:324–32.
19. Walter SD, Ishikawa H, Galetta KM, Sakai RE, Feller DJ, Henderson SB, et al. Ganglion cell loss in relation to visual disability in multiple sclerosis. Ophthalmology. 2012;119:1250–7.
20. Saidha S, Syc SB, Durbin MK, Eckstein C, Oakley JD, Meyer SA, et al. Visual dysfunction in multiple sclerosis correlates better with optical coherence tomography derived estimates of macular ganglion cell layer thickness than peripapillary retinal nerve fiber layer thickness. Mult Scler. 2011;17:1449–63.
21. Narayanan D, Cheng H, Bonem KN, Saenz R, Tang RA, Frishman LJ. Tracking changes over time in retinal nerve fiber layer and ganglion cell-inner plexiform layer thickness in multiple sclerosis. Mult Scler. 2014;20(10):1331–41.
22. Garcia-Martin E, Pueyo V, Martin J, Almarcegui C, Ara JR, Dolz I, et al. Progressive changes in the retinal nerve fiber layer in patients with multiple sclerosis. Eur J Ophthalmol. 2010;20:167–73.
23. Petzold A, Balcer LJ, Calabresi PA, Costello F, Frohman TC, Frohman EM, et al. Retinal layer segmentation in multiple sclerosis: a systematic review and meta-analysis. Lancet Neurol. 2017;16:797–812.
24. Gabilondo I, Sepúlveda M, Ortiz-Perez S, Graga-Pumar E, Martínez-Lapiscina EH, Llufriu S, et al. Retrograde retinal damage after acute optic tract lesion in MS [letter]. J Neurol Neurosurg Psychiatry. 2013;84:824–6.
25. Saidha S, Al-Louzi O, Ratchford JN, Bhargava P, Oh J, Newsome SD, et al. Optical coherence tomography reflects brain atrophy in multiple sclerosis: a four-year study. Ann Neurol. 2015;78:801–13.
26. Abalo-Lojo JM, Limeres CC, Gómez MA, Baleato-González S, Cadarso-Suárez, Capeáns-Tomé C, et al. Retinal nerve fiber layer thickness, brain atrophy, and disability in multiple sclerosis patients. J Neuroophthalmol. 2014;34:23–28.
27. Oh J, Sotirchos ES, Saidha S, Whetstone A, Chen M, Newsome SD, et al. Relationships between quantitative spinal cord MRI and retinal layers in multiple sclerosis. Neurology. 2015;84:720–8.
28. Garcia-Martin E, Ara JR, Martin J, Almarcegui C, Dolz I, Vilades E, et al. Retinal and optic nerve degeneration in patients with multiple sclerosis followed up for 5 years. Ophthalmology. 2017;124:688–96.
29. Ratchford JN, Saidha S, Sotirchos ES, Oh JA, Seigo MA, Eckstein C, et al. Active MS is associated with accelerated retinal ganglion cell/inner plexiform layer thinning. Neurology. 2013;80:47–54.
30. Rothman A, Murphy OC, Fitzgerald KC, Button J, Gordon-Lipkin E, Ratchford JN, et al. Retinal measurements predict 10-year disability in multiple sclerosis. Ann Clin Transl Neurol. 2019;6:222–32.
31. Gelfand JM, Nolan R, Schwarz DM, Graves J, Green AJ. Microcystic macular oedema in multiple sclerosis is associated with disease severity. Brain. 2012;135:1786–93.
32. Saidha S, Sotirchos ES, Ibrahim MA, Crainiceanu CM, Gelfand JM, Sepah YJ, et al. Microcystic macular oedema, thickness of the inner nuclear layer of the retina, and disease characteristics in multiple sclerosis: a retrospective study. Lancet Neurol. 2012;11:963–72.
33. Wolff B, Azar G, Vasseur V, Sahel JA, Vignal C, Mauget-Faÿsse M. Microcystic changes in the retinal internal nuclear layer associated with optic atrophy: a prospective study. J Ophthalmol. 2014;2014:395189.
34. Barboni P, Carelli V, Savini G, Carbonelli M, La Morgia C, Sadun AA. Microcystic macular degeneration from optic neuropathy: not inflammatory, not trans-synaptic degeneration. Brain. 2013;136:e239.
35. Wolff B, Basdekidou C, Vasseur V, Mauget-Faÿsse M, Sahel JA, Vignal C. Retinal inner nuclear layer microcystic changes in optic nerve atrophy: a novel spectral-domain OCT finding. Retina. 2013;33:2133–8.
36. Pott JWR, de Vries-Knoppert WAEJ, Petzold A. The prevalence of microcystic macular changes on optical coherence tomography of the macular region in optic nerve atrophy of non-neuritis origin: a prospective study. Br J Ophthalmol. 2016;100:216–21.
37. Bennett JL, de Seze J, Lana-Peixoto M, Waldman A, Schippling S, Tenembaum S, et al. Neuromyelitis optica and multiple sclerosis: Seeing differences through optical coherence tomography. Mult Scler. 2015;21:678–88.

38. Ratchford JN, Quigg ME, Conger A, Frohman E, Balcer LJ, Calabresi PA, et al. Optical coherence tomography helps differentiate neuromyelitis optica and MS optic neuropathies. Neurology 2009;73:302–8.
39. Manogaran P, Traboulsee AL, Lange A. Longitudinal study of retinal nerve fiber layer thickness and macular volume in patients with neuromyelitis optica spectrum disorder. J Neuroophthalmol. 2016;36:363–8.
40. Pisa M, Ratti F, Vabanesi M, Radaelli M, Guerrieri S, Moiola L, et al. Subclinical neurodegeneration in multiple sclerosis and neuromyelitis optica spectrum disorder revealed by optical coherence tomography. Mult Scler. 2020;26:1196–206.
41. Oertel FC, Outteryck O, Knier B, Zimmermann H, Borisow N, Bellmann-Strobl J, et al. Optical coherence tomography in myelin-oligodendrocyte-glycoprotein antibody-seropositive patients: a longitudinal study. J Neuroinflammation. 2019;16:154.
42. Balk LJ, Killestein J, Polman C, Uitdehaag BMJ, Petzold A. Microcystic macular oedema confirmed, but not specific for multiple sclerosis [letter]. Brain. 2012;135:e226.
43. Schneider E, Zimmermann H, Oberwahrenbrock T, Kaufhold F, Kadas EM, Petzold A, et al. Optical coherence tomography reveals distinct patterns of retinal damage in neuromyelitis optica and multiple sclerosis. PLoS ONE. 2013;8:e66151.
44. Fernandes DB, Raza AS, Nogueira RG, Wang D, Callegaro D, Hood DC, et al. Evaluation of inner retinal layers in patients with multiple sclerosis or neuromyelitis optica using optical coherence tomography. Ophthalmology. 2013;120:387–94.
45. Hamann S, Malmqvist L, Costello F. Optic disc drusen: understanding an old problem from a new perspective. Acta Ophthalmol. 2018;96:673–84.
46. Chen JJ, Costello F. The role of optical coherence tomography in neuro-ophthalmology. Ann Eye Sci. 2018;3:35.
47. Lee KM, Woo SJ, Hwang JM. Differentiation of optic nerve head drusen and optic disc edema with spectral domain optical coherence tomography. Ophthalmology. 2011;228:971–7.
48. Bassi ST, Mohana KP. Optical coherence tomography in papilledema and pseudopapilledema with and without optic nerve head drusen. Indian J Ophthalmol. 2014;62:1146–51.
49. Kulkarni KM, Pasol J, Rosa PR, Lam BL. Differentiating mild papilledema and buried optic nerve head drusen using spectral domain optical coherence tomography. Ophthalmology. 2014;121:959–63.
50. Johnson LN, Diehl ML, Hamm CW, Sommerville DN, Petroski GF. Differentiating optic disc edema from optic nerve head drusen on optical coherence tomography. Arch Ophthalmol. 2009;127:45–9.
51. Sarac O, Tasci YY, Gurdal C, Can I. Differentiation of optic disc edema from optic nerve head drusen with spectral-domain optical coherence tomography. J Neuroophthalmol. 2012;32:207–11.
52. Malmqvist L, Bursztyn L, Costello F, Digre K, Fraser JA, Fraser C, et al. The optic disc drusen studies consortium recommendations for diagnosis of optic disc drusen using optical coherence tomography. J Neuroophthalmol. 2018;38:299–307.
53. Merchant KY, Su D, Park SC, Qayum S, Banik R, Liebmann JM, et al. Enhanced depth imaging optical coherence tomography of optic nerve head drusen. Ophthalmology. 2013;120:1409–14.
54. Traber GL, Weber KP, Sabah M, Keane PA, Plant GT. Enhanced depth imaging optical coherence tomography of optic nerve head drusen: a comparison of cases with and without visual field loss. Ophthalmology. 2017;124:66–73.
55. Skaat A, Muylaert S, Mogil RS, Furlanetto RL, Netto CF, Banik R, et al. Relationship between optic nerve head drusen volume and structural and functional optic nerve head damage. J Glaucoma. 2017;26:1095–100.
56. Corbett JJ, Savino PJ, Thompson HS, Kansu T, Schatz NJ, Orr LS, et al. Visual loss in pseudotumour cerebri. Follow-up of 57 patients from five to 41 years and a profile of 14 patients with permanent severe visual loss. Arch Neurol. 1982;39:461–74.
57. Scott CJ, Kardon RH, Lee AG, Frisén L, Wall M. Diagnosis and grading of papilledema in patients with raised intracranial pressure using optical coherence tomography vs clinical expert assessment using a clinical staging scale. Arch Ophthalmol. 2010;128:705–11.
58. Sinclair AJ, Burdon MA, Nightingale PG, Matthews TD, Jacks A, Lawden M, et al. Rating papilloedema: an evaluation of the Frisén classification in idiopathic intracranial hypertension. J Neurol. 2012;259:1406–12.
59. Kupersmith MJ, Sibony P, Mandel G, Durbin M, Kardon RH. Optical coherence tomography of the swollen optic nerve head: deformation of the peripapillary retinal pigment epithelium layer in papilledema. Invest Ophthalmol Vis Sci. 2011;52:6558–64.
60. Sibony P, Kupersmith MJ, Rohlf FJ. Shape analysis of the peripapillary RPE layer in papilledema and ischemic optic neuropathy. Invest Ophthalmol Vis Sci. 2011;52:7987–95.
61. Sibony P, Kupersmith MJ, Honkanen R, Rohlf FJ, Torab-Parhiz A. Effects of lowering cerebrospinal fluid pressure on the shape of the peripapillary retina in intracranial hypertension. Invest Ophthalmol Vis Sci. 2014;55:8223–31.
62. Gampa A, Vangipuram G, Shirazi Z, Moss HE. Quantitative association between peripapillary Bruch's membrane shape and intracranial pressure. Invest Ophthalmol Vis Sci. 2017;58:2739–45.
63. Anand A, Pass A, Urfy MZ, Tang R, Cajavilca C, Calvillo E, et al. Optical coherence tomography of the optic nerve head detects acute changes in intracranial pressure. J Clin Neurosci. 2016;29:73–6.
64. Hoye VJ 3rd, Berrocal AM, Hedges TR 3rd, Amaro-Quireza ML. Optical coherence tomography demonstrates subretinal macular edema from papilledema. J Clin Neurosci. 2016;29:73–6.
65. Dotan G, Goldstein M, Kesler A, Skarf B. Long-term retinal nerve fiber layer changes following nonarteritic anterior ischaemic optic neuropathy. Clin Ophthalmol. 2013;7:735–40.
66. Contreras I, Rebolleda G, Noval S, Muñoz-Negrete FJ. Optic disc evaluation by optical coherence tomography in nonarteritic anterior ischaemic optic neuropathy. Invest Ophthalmol Vis Sci. 2007;48:4087–92.
67. Contreras I, Rebolleda G, Noval S, Muñoz-Negrete FJ. Ischemic optic neuropathy. Ophthalmology. 2009;116:814.
68. De Dompablo E, Garcia-Montesinos J, Munoz-Negrete FJ, Rebolleda G. Ganglion cell analysis at acute episode of non-arteritic anterior ischemic optic neuropathy to predict irreversible damage. A prospective study. Graefes Arch Clin Exp Ophthalmol. 2016;254:1793–800.
69. Kernstock C, Beisse F, Wiethoff S, Mast A, Krapp E, Grund R, et al. Assessment of functional and morphometric endpoints in patients with non-arteritis anterior ischemic optic neuropathy (NAION). Graefes Arch Clin Exp Ophthalmol. 2014;252:515–21.
70. Papchenko T, Grainger BT, Savino PJ, Gamble GD, Danesh-Meyer HV. Macular thickness predictive of visual field sensitivity in ischaemic optic neuropathy. Acta Ophthalmol. 2012;90:463–9.
71. Gonul S, Koktekir BE, Bakbak B, Gedik S. Comparison of the ganglion cell complex and retinal nerve fiber layer measurements using Fourier domain optical coherence tomography to detect ganglion cell loss in non-arteritis anterior ischaemic optic neuropathy. Br J Ophthalmol. 2013;97:1045–50.
72. Zhang Y, Ye Z, Wang M, Qiao N. Ganglion cell complex loss precedes retinal nerve fiber layer thinning in patients with pituitary adenoma. J Clin Neurosci. 2017;43:274–7.
73. Monteiro MLR. Macular ganglion cell complex reduction preceding visual field loss in a patient with chiasmal compression with a 21-month follow-up. J Neuroophthalmol. 2018;38:124–7.

74. Tieger MG, Hedges TR3rd, Ho J, Erlich-Malona NK, Vuong LN, Athappilly GK. Ganglion cell complex loss in chiasmal compression by brain tumours. J Neuroophthalmol. 2017;37:7–12.
75. Unsold R, Hoyt WF. Band atrophy of the optic nerve. The histology of temporal hemianopsia. Arch Ophthalmol. 1980;98:1637–8.
76. Monteiro ML, Leal BC, Rosa AA, Bronstein MD. Optical coherence tomography analysis of axonal loss in band atrophy of the optic nerve. Br J Ophthalmol. 2004;88:896–9.
77. Kanamori A, Nakamura M, Matsui N, Nagai A, Nakanishi Y, Kusuhara S, et al. Optical coherence tomography detects characteristic retinal nerve fiber layer thickness corresponding to band atrophy of the optic discs. Ophthalmology. 2004;111:2278–83.
78. Danesh-Meyer HV, Carroll SC, Foroozan R, Savino PJ, Fan J, Jiang Y, et al. Relationship between retinal nerve fiber layer and visual field sensitivity as measured by optical coherence tomography in chiasmal compression. Invest Ophthalmol Vis Sci. 2006;47:4827–35.
79. Costa-Cunha LV, Cunha LP, Malta RF, Monteiro MLR. Comparison of Fourier-domain and time-domain optical coherence tomography in the detection of band atrophy of the optic nerve. Am J Ophthalmol. 2009;147:56–63.e2.
80. Monteiro ML, Cunha LP, Vessani RM. Comparison of retinal nerve fiber layer measurements using Stratus OCT fast and regular scan protocols in eyes with band atrophy of the optic nerve and normal controls. Arq Bras Oftalmol. 2008;71:534–9.
81. Sun M, Zhang A, Ma C, Chin S, Chen X. Quantitative analysis of retinal layers on three-dimensional spectral-domain optical coherence tomography for pituitary adenoma. PLoS ONE. 2017;12:e0179532.
82. Yum HR, Park SH, Park HY, Shin SY. Macular ganglion cell analysis determined by cirrus HD optical coherence tomography for early detecting chiasmal compression. PLoS ONE. 2016;11:e0153064.
83. Zehnder S, Wildberger H, Hanson JVM, Lukas S, Pelz S, Landau K, et al. Retinal ganglion cell topography in patients with visual pathway pathology. J Neuroophthalmol. 2018;38:172–8.
84. Dinkin M. Trans-synaptic retrograde degeneration in the human visual system: slow, silent, and real. Curr Neurol Neurosci Rep. 2017;17:16.
85. Fisher MJ, Loguidice M, Gutmann DH, Listernick R, Ferner RE, Ullrich NJ, et al. Visual outcomes in children with neurofibromatosis type I-associated optic pathway glioma following chemotherapy: a multicenter retrospective analysis. Neuro Oncol. 2012;14:790–7.
86. Avery RA, Cnaan A, Schuman JS, Trimboli-Heidler C, Chen CL, Packer RJ, et al. Longitudinal change of circumpapillary retinal fiber layer thickness in children with optic pathway gliomas. Am J Ophthalmol. 2015;160:944–52.
87. Avery RA, Mansoor A, Idrees R, Trimboli-Heidler C, Ishikawa H, Packer RJ, et al. Optic pathway glioma volume predicts retinal axon degeneration in neurofibromatosis type 1. Neurology. 2016;87:2403–7.
88. Yoneoka Y, Hatase T, Watanabe N, Jinguji S, Okada M, Takagi M, et al. Early morphological recovery of the optic chiasm is associated with excellent visual outcome in patients with compressive chiasmal syndrome caused by pituitary tumors. Neurol Res. 2015;37:1–8.
89. Ohkubo S, Higashide T, Takeda H, Murotani E, Hayashi Y, Sugiyama K. Relationship between macular ganglion cell complex parameters and visual field parameters after tumor resection in chiasmal compression. Jpn J Ophthalmol. 2012;56:68–75.
90. Moon CH, Hwang SC, Kim BT, Ohn YH, Park TK. Visual prognostic value of optical coherence tomography and photopic negative response in chiasmal compression. Invest Ophthalmol Vis Sci. 2011;52:8527–33.
91. Matsunaga D, Yi J, Puliafito CA, Kashani AH. OCT angiography in healthy human subjects. Osli Retin 2014;45:510–5.
92. Mase T, Ishibazawa A, Nagaoka T, Yokota H, Yoshida A. Radial peripapillary capillary network visualized using wide-field montage optical coherence tomography angiography. Invest Ophth Vis Sci. 2016;57:OCT504–10.
93. Bojikian KD, Chen CL, Wen JC, Zhang QQ, Xin C, Gupta D, et al. Optic disc perfusion in primary open angle and normal tension glaucoma eyes using optical coherence tomography-based microangiography. PLoS ONE. 2016;11:e0154691.
94. Wang XG, Jia YL, Spain R, Potsaid B, Liu JJ, Baumann B, et al. Optical coherence tomography angiography of optic nerve head and parafovea in multiple sclerosis. Brit J Ophthalmol. 2014;98:1368–73.
95. Hata M, Oishi A, Muraoka Y, Miyamoto K, Kawai K, Yokota S, et al. Structural and functional analyses in nonarteritic anterior ischemic optic neuropathy: optical coherence tomography angiography study. J Neuro-Ophthalmol. 2017;37:140–8.
96. Sharma S, Ang M, Najjar RP, Sng C, Cheung CY, Rukmini AV, et al. Optical coherence tomography angiography in acute nonarteritic anterior ischaemic optic neuropathy. Brit J Ophthalmol. 2017;101:1045–51.
97. Gaier ED, Gilbert AL, Cestari DM, Miller JB. Optical coherence tomographic angiography identifies peripapillary microvascular dilation and focal non-perfusion in giant cell arteritis. Brit J Ophthalmol. 2018;102:1141–6.
98. Balducci N, Cascavilla ML, Ciardella A, La Morgia C, Triolo G, Parisi V, et al. Peripapillary vessel density changes in Leber's hereditary optic neuropathy: a new biomarker. Clin Exp Ophthalmol. 2018;46:1055–62.
99. De Rojas JO, Rasool N, Chen RWS, Horowitz J, Odel JG. Optical coherence tomography angiography in Leber hereditary optic neuropathy. Neurology. 2016;87:2065–6.